

Global Biogeochemical Cycles

RESEARCH ARTICLE

10.1029/2017GB005863

Key Points:

- Cycling and budgets of organic and black carbon in both particulate and dissolved phases in a coastal sea were investigated
- Both natural and anthropogenic perturbations exerted significant impacts on organic and black carbon cycling and budgets in Bohai Sea
- Regional/global databases demonstrate that future studies should calculate particulate and dissolved black carbon fluxes independently

Supporting Information:

- Supporting Information S1
- Figure S1
- Figure S2
- Figure S3
- Figure S4
- Data Set S1
- Data Set S2
- Data Set S3

Correspondence to:

Y. Chen, C. Tian, and T. Lin,
 yjchentj@tongji.edu.cn;
 cgtian@yic.ac.cn;
 lintian@vip.gyig.ac.cn

Citation:

Fang, Y., Chen, Y., Tian, C., Wang, X., Lin, T., Hu, L., et al. (2018). Cycling and budgets of organic and black carbon in coastal Bohai Sea, China: Impacts of natural and anthropogenic perturbations. *Global Biogeochemical Cycles*, 32, 971–986. <https://doi.org/10.1029/2017GB005863>

Received 11 DEC 2017

Accepted 7 MAY 2018

Accepted article online 12 MAY 2018

Published online 15 JUN 2018

©2018. American Geophysical Union.
 All Rights Reserved.

Cycling and Budgets of Organic and Black Carbon in Coastal Bohai Sea, China: Impacts of Natural and Anthropogenic Perturbations

Yin Fang^{1,2} , Yingjun Chen^{1,3} , Chongguo Tian⁴ , Xiaoping Wang², Tian Lin⁵ , Limin Hu^{6,7}, Jun Li² , Gan Zhang², and Yongming Luo⁴

¹Key Laboratory of Cities' Mitigation and Adaptation to Climate Change in Shanghai, College of Environmental Science and Engineering, Tongji University, Shanghai, China, ²State Key Laboratory of Organic Geochemistry, Guangzhou Institute of Geochemistry, Chinese Academy of Sciences, Guangzhou, China, ³Shanghai Institute of Pollution Control and Ecological Security, Shanghai, China, ⁴Key Laboratory of Coastal Environmental Processes and Ecological Remediation, Yantai Institute of Coastal Zone Research, Chinese Academy of Sciences, Yantai, China, ⁵State Key Laboratory of Environmental Geochemistry, Guiyang Institute of Geochemistry, Chinese Academy of Sciences, Guiyang, China, ⁶Key Laboratory of Marine Sedimentology and Environmental Geology, First Institute of Oceanography, State Oceanic Administration, Qingdao, China, ⁷Laboratory for Marine Geology, Qingdao National Laboratory for Marine Science and Technology, Qingdao, China

Abstract Organic carbon (OC) cycling in coastal seas that connect terrestrial and open oceanic ecosystems is a dynamic and disproportionately important component of oceanic and global carbon cycles. However, OC cycling in coastal seas needs to be better constrained, particularly for geochemically important black carbon (BC). In this study, we conducted multimedium sampling campaigns, including atmospheric deposition, river water, seawater, and sediments in coastal Bohai Sea (BS) in China. We simultaneously quantified particulate OC (POC), particulate BC (PBC), dissolved OC (DOC), and dissolved BC (DBC) and investigated the cycling and budgets of OC and BC. The cycling and budgets of each individual particulate phase (i.e., POC versus PBC) and dissolved phase (i.e., DOC versus DBC) displayed similar patterns, but there were some distinct differences between the particulate and dissolved phases. In the particulate phases, atmospheric and riverine delivery dominated exogenous inputs (>80%), sequestration to sediments dominated removal (~70%), and exchanges in the Bohai Strait resulted in net export. In the dissolved phases, exchanges in the Bohai Strait dominated both import and export and were in a relatively dynamic equilibrium. We found that both natural perturbations, such as spring dust storms, and anthropogenic activity, exerted significant impacts on BS carbon cycling. The integration of regional and global source-to-sink process databases made it clear that future BC studies should calculate PBC and DBC fluxes independently. Continuous field observational studies, more details of the biogeochemical processes involved, and consistent BC quantification methods are urgently needed to elucidate coastal OC and BC cycling.

1. Introduction

Coastal seas are geographically pivotal transition zones that connect terrestrial and open oceanic ecosystems. Organic carbon (OC) cycling in coastal seas is a dynamic and disproportionately important component in the context of oceanic and global carbon cycles and budgets (Bauer et al., 2013). It has been estimated that despite comprising only 7%–10% of the global ocean, coastal seas account for 20%–30% of global marine primary productivity, 80%–90% of OC accumulation in sediments, and up to 50% of biological pump transfer of OC to the open ocean (Bauer et al., 2013; Bianchi et al., 2014; Liu et al., 2010). Black carbon (BC), also termed elemental carbon (EC) and pyrogenic carbon (PyC) (Santin et al., 2015; Wiedemeier et al., 2013), is the byproduct derived exclusively from incomplete combustion of fossil fuels and biomass. It constitutes a significant fraction of OC and has received considerable attention due to its physical and chemical properties being remarkably different from those of other fractions of OC. As a result, the roles of BC differ from those of OC in a wide range of biogeochemical processes, such as the regional/global carbon cycle (Bird et al., 2015; Guo et al., 2004; Sánchez-García et al., 2012), climate change (Menon et al., 2002; Ramanathan & Carmichael, 2008), sorption of toxic pollutants, and bioavailability/fate (Dutta et al., 2017). It is therefore of great necessity to calculate and compare OC and BC fluxes independently and to determine the factors that regulate these fluxes in coastal regimes accurately. This will lead to a more comprehensive understanding of oceanic and global carbon cycling.

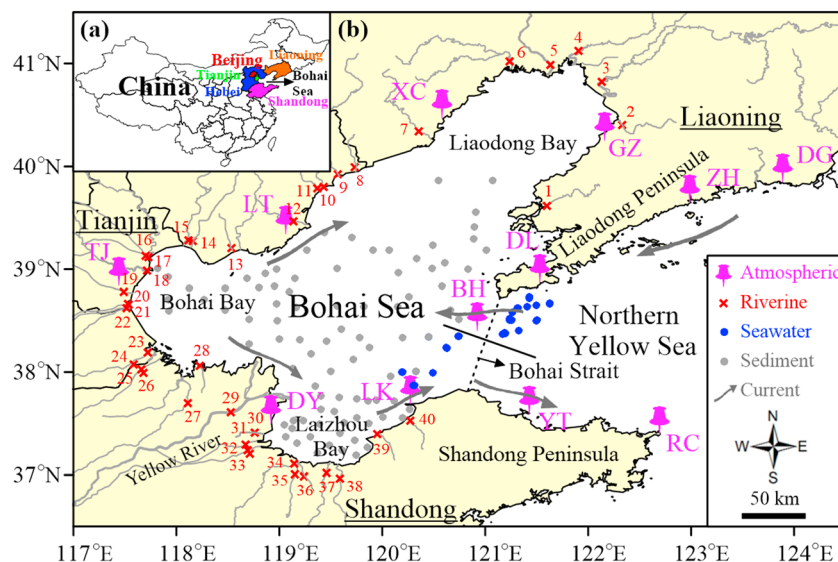


Figure 1. Map showing the study area and sampling sites. (a) The shaded area in Figure 1a denotes provinces/municipalities in Bohai Rim, including Liaoning, Hebei, Shandong, Beijing, and Tianjin. (b) Abbreviations in Figure 1b for coastal atmospheric deposition sampling sites (pink) are DG (DongGang), ZH (ZhuangHe), DL (DaLian), GZ (GaiZhou), XC (XingCheng), LT (LaoTing), TJ (TianJin), DY (DongYing), LK (LongKou), YT (YanTai), RC (RongCheng), and BH (BeichengHuangdao). (c) The ocean currents in Figure 1b refer to Hu et al. (2011)).

Owing to rapid economic development and associated high-energy consumption in China in recent decades, there have been numerous studies of anthropogenic OC and BC emissions and their relevant effects (Bond et al., 2004; Cao et al., 2006; Menon et al., 2002; Peng et al., 2016; R. Wang et al., 2012). The OC and BC emission inventories indicate that regions in Bohai Rim, including the three provinces of Liaoning, Hebei, and Shandong and the two municipalities of Beijing and Tianjin (Figure 1a), have the highest emission intensities in China. These regions contribute >20% of China's total emissions of both OC and BC, despite accounting for only 5% of Chinese territory. Significant amounts of the anthropogenic OC and BC are readily transported to the coastal Bohai Sea (BS) and subsequently participate in the coastal BS carbon cycle, owing to the combined influences of the northwesterly prevailing winter, spring East Asian monsoon, and high riverine discharge, including that of the Yellow River, which yields the world's second largest riverine sediment flux into the ocean (Hu et al., 2016). Concurrently, extreme natural weather events, such as frequent and intense spring dust storms that occur in northern China (Chen et al., 2017; Wang et al., 2017), can deliver dust particles and particle-bound OC and BC into the BS following long-range transport. Tan et al. (2012) reported that the total deposition of dust particles for the days on which dust storms affected Chinese seas was ~36 million tons, which was equivalent to ~5% of the total emission of spring dust storms in Inner Mongolia during 2000–2007. The OC and BC in BS is sequestered in sediments due to relatively weak hydrodynamic conditions and is also exported to other coastal seas (e.g., the Northern Yellow Sea, NYS) and open oceans (e.g., the Northwest Pacific Ocean) through the narrow eastern Bohai Strait. The BS is therefore an ideal target area to study coastal OC and BC cycling and budgets.

There have been many studies of OC and BC in the atmosphere, soils, riverine and oceanic waters, and sediments in Bohai Rim (Andersson et al., 2015; Fang et al., 2015; Hu et al., 2016; G. Huang et al., 2016; Kang et al., 2009; Li et al., 2016; Wang et al., 2016; Xu et al., 2016; Zhang et al., 2013). However, most have focused either on part of the OC and BC fractions (i.e., only OC or BC or a single particulate or dissolved phase) or on a single environmental compartment, resulting in a lack of investigation of the integration of coastal BS carbon cycling and budgets. To address this geochemically important issue, we conducted multimedium sampling campaigns that included sampling of atmospheric deposition, river water, seawater, and marine sediments. We quantified both particulate and dissolved phases of OC and BC, including particulate OC (POC), particulate BC (PBC), dissolved OC (DOC), and dissolved BC (DBC). Among these, the DBC flux and cycling remain the most poorly constrained (Bao et al., 2017; Fang et al., 2017; Jaffé et al., 2013; Masiello & Louchouart, 2013). This study had three major objectives: (1) to calculate each process-based OC and BC

flux in coastal BS, (2) to identify the impacts of natural and anthropogenic perturbations on the temporal and/or spatial regulation of these fluxes, and (3) to construct coastal BS OC and BC cycling and budgets. From a global perspective, this study will also provide an essential database and information for future coastal and global ocean carbon cycling assessments.

2. Materials and Methods

2.1. Sample Collection and Preparation

Atmospheric deposition, riverine discharge, exchange in the Bohai Strait, and sinking to sediments are major processes associated with the BS carbon cycle. The sampling sites for calculations of these process-based fluxes are illustrated in Figure 1.

For atmospheric deposition, both particulate and dissolved samples were collected over a year-round period from June 2014 to May 2015 at a frequency of three consecutive months (summer: June–August; autumn: September–November; winter: December–February; and spring: March–May) at 12 coastal sites in Bohai Rim. The particulate phase was achieved in situ by self-designed stainless steel atmospheric deposition sampler with a receiving area of 0.049 m². A 45-mm-diameter quartz fiber filter (QFF, Whatman, nominal pore size 0.7 μm) for retaining the particulate phase was placed in a blinded screen housing. After collection, it was packed with prefired aluminum foil. For the dissolved phase, a 2-L Teflon bottle attached to a cylindrical polyethylene plastic tube with a receiving area of 0.0095 m² was used for collecting the bulk deposition. The dissolved phase was separated from particulate phase via filtering the bulk deposition through QFF in the laboratory. The particulate and dissolved phases were stored at –20 °C for further analysis. Here it should be noted that the atmospheric deposition of OC and BC is likely an underestimate due to possible photodegradation during the 3-month-long collecting time (Stubbins et al., 2012).

For riverine discharge, four sampling campaigns (August 2013; March, August, and October 2014) with different water discharge rates were conducted on 40 rivers in Bohai Rim, including the most concerned Yellow River (No. 29, Figure 1b). The riverine water sampling sites were selected not to be affected by the intruded seawater. For exchange in the Bohai Strait, previous observation and numerical simulation showed that the water exchange in the Bohai Strait generally shows features with water flowing into the BS through the northern Bohai Strait and flowing out of the BS through the southern Bohai Strait (Bi et al., 2011). Therefore, the sites located to the east of the northern Bohai Strait and to the west of the southern Bohai Strait were strategically deployed to collect seawater samples for calculations of import fluxes from NYS to BS and export fluxes from BS to NYS, respectively. Considering the large temporal and vertical variations of carbon concentrations, the seawater samples were collected over different seasons (April and September 2010, June and November 2011, and August and December 2014) and layers (surface, middle, and bottom). Upon retrieval of the riverine and seawater samples, they were immediately filtered through precombusted and weighed 47 mm diameter QFF in the hotel or in situ on board to separate between the particulate and dissolved phases. The particulate phase was reweighed and stored at –20 °C for following analysis. For the dissolved phase, aliquots of 40 mL were kept in prebaked amber glass bottles at 4 °C for DOC determination. In addition, aliquots of 1 L were acidified with concentrated HCl (32%) to pH = 2. The acidified water was extracted for dissolved organic matter (DOM, containing DBC) with prerinsed (10 mL of methanol, HPLC grade) solid phase extraction (SPE) cartridges (Supelco Supelclean ENVI-Chrom P, 500 mg; G. Huang et al., 2016). After extraction, the cartridges were desalted with 20 mL of acidified water (pH = 2), dried under an air stream, and stored at –20 °C for DBC quantification. For sinking to sediments, the sediment sampling and analytical procedures are detailed in our recent work (Fang et al., 2015). A total of 89 surface sediment samples (0–3 cm), covering >80% of the BS area, were sampled (Figure 1b).

2.2. Analytical Procedures

2.2.1. POC and PBC Analysis

Due to overwhelmingly high loadings of PM and their uneven distributions onto the filters, a tiny fraction of samples (0.5–3.0 mg) were gingerly scraped and smeared as even as possible onto 0.544 cm² prefired QFFs. The QFFs loaded with PM and riverine and seawater total suspended solids (TSS) were acidified with concentrated HCl fumes (32%) for 24 hr to thoroughly remove the inorganic carbon. Thereafter, they were analyzed for POC and PBC on a Desert Research Institute (DRI) Model 2001 Thermal/Optical Carbon Analyzer (Atmoslytic Inc., Calabasas, CA) following the Interagency Monitoring of Protected Visual Environment (IMPROVE) protocol (Cong et al., 2013; Fang et al., 2015; Han et al., 2007). During the carbon analysis, the

oven was first heated in 100% He atmosphere, producing four OC subfractions (OC1, OC2, OC3, and OC4) in four temperature steps (140, 280, 480, and 580 °C). The atmosphere was then shifted to 2% O₂/98% He, and correspondingly, three BC subfractions (BC1, BC2, and BC3) were produced at three temperature steps (580, 740, and 840 °C). Pyrolysis of organic carbon (defined as OCP_{yro}) occurred in 100% He atmosphere, as indicated by the decreased reflectance signal of the laser. OCP_{yro} similar to the original BC component was oxidized in the second O₂/He stage. The IMPROVE protocol defined POC as the sum of all OC and BC subfractions (i.e., POC = OC1 + OC2 + OC3 + OC4 + BC1 + BC2 + BC3), and PBC as the sum of three BC subfractions minus the OCP_{yro} (i.e., PBC = BC1 + BC2 + BC3 – OCP_{yro}).

2.2.2. DOC Analysis

DOC in atmospheric deposition-dissolved phase, river water, and seawater was quantified using a high-temperature catalytic oxidation (HTCO) method on a total organic carbon analyzer (TOC-V_{CPH}, Shimadzu Corporation, Japan) equipped with an AIS-V autosampler. Samples were oxidized in a furnace at 680 °C with the preconditioned platinum catalyst. The combustion-derived CO₂ was carried by ultrahigh purity O₂ (99.999%) and detected by a nondispersive infrared (NDIR) detector. The accuracy was checked daily against low-carbon water and deep Atlantic seawater reference materials (D.A. Hansell, University of Miami, Florida). Procedural blanks, including the filtration process, were obtained using the ultrapure water. The blank samples contained nondetectable DOC concentrations. Relative standard deviation (RSD, %) of DOC analysis was within 5% for duplicates.

2.2.3. DBC Analysis

DBC in riverine and seawater samples was determined at the molecular level via benzene polycarboxylic acids (BPCAs) method recently optimized in our group (G. Huang et al., 2016). DBC from the cartridges was eluted with 10 mL of methanol. The extract was condensed to nearly dryness (~0.5 mL) with high-purity N₂ stream at 50 °C. It was then transferred into 2 mL Teflon digestion tube. After redrying in the tube, 0.5 mL of concentrated HNO₃ (65%) was added. The tube was sealed and heated at 170 °C for 7 hr in an oven for converting DBC into the molecular markers of BPCAs. After digestion, the remaining HNO₃ and water was evaporated under a stream of high-purity N₂ at 50 °C. The digestion product was redissolved in 1 mL of methanol/water mixture (50:50, V/V), and 10 µg of biphenyl-2'-2-dicarboxylic acid (2 µg/µL in methanol) was added as an internal standard. The sample was transferred into the high-performance liquid chromatography (HPLC) system autosampler vial for BPCAs analysis.

The BPCAs were quantified on a Waters Alliance E2695 HPLC system equipped with an autosampler and a photodiode array (PDA) light absorbance detector. A Phenomenex Synergi Polar RP column (4.6 × 250 mm, 4 µm) and a binary gradient consisting of mobile phase A (0.5% formic acid in water, V/V) and B (methanol) were used to achieve the chromatographic separation. The BPCAs were identified by the retention time and absorbance spectra (210–400 nm), and quantification was conducted using the absorbance signal at 240 nm. The retention time was stable and reproducible, and it was within 1 min during 3 months of routine analysis using the same HPLC column. The detection limit was 5 ng per injection. The recovery of BPCAs was complete during the whole analytical steps, including digestion, as determined from a BPCA standard solution. Blank sample analysis showed no detectable target compounds. RSD for BPCAs analysis was on average <5% for duplicates (G. Huang et al., 2016).

In this study, all BPCAs (including seven nitro-BPCAs) with three or more carboxyl functional groups (-COOH) were operationally defined as DBC. The B2CAs (substituted with two -COOH) were not included, because they might be derived from processes other than incomplete combustion, such as lignin and humic substances (Brodowski et al., 2005; Coppola et al., 2014). Some target compounds with standards commercially unavailable were quantified by the analogous standard compounds calibration curves. For instance, the curve of 5-nitro-1,2,3-B3CA was used to quantify all nitro-B3CAs (five compounds), and the curve of 1,2,4,5-B4CA was used to quantify 1,2,3,4-B4CA, 1,2,3,5-B4CA, and two nitro-B4CAs (G. Huang et al., 2016). A conversion factor of 25.7 ± 6.8% C was used to convert BPCAs-C to DBC-C for the original riverine and seawater samples (i.e., DBC-C = 4.0 BPCAs-C) (Ziolkowski et al., 2011).

2.3. Calculations of Each Process-Based Flux

To achieve a comprehensive understanding of BS carbon cycle, the primary step is to calculate each process-based flux, consisting of atmospheric deposition, riverine export, exchange in the Bohai Strait, and sinking to sediments.

2.3.1. Atmospheric Depositional Fluxes

2.3.1.1. Atmospheric Particulate Phase Depositional Fluxes

The daily atmospheric particulate phase depositional fluxes were calculated as follows:

$$f_{PM_i}^A = m_i / (A \times t_i) \quad (1)$$

$$f_{POC_i}^A = f_{PM_i}^A \times (C_{POC_i}^A / 10^3) \quad (2)$$

$$f_{PBC_i}^A = f_{PM_i}^A \times (C_{PBC_i}^A / 10^3) \quad (3)$$

where $f_{PM_i}^A$, $f_{POC_i}^A$, and $f_{PBC_i}^A$ are the PM, POC, and PBC daily atmospheric particulate phase depositional fluxes ($\text{mg} \cdot \text{m}^{-2} \cdot \text{d}^{-1}$) in *i* season at each sampling site, respectively. *A* is the area (m^2) of the stainless steel funnel receiving particulate phase samples. The parameter t_i is the actual sampling duration (days) in *i* season. The parameter m_i is the corresponding mass of PM (mg) deposited onto the filter during t_i sampling duration. $C_{POC_i}^A$ and $C_{PBC_i}^A$ are the mass concentrations of POC and PBC (mg/g) in *i* season, respectively. The 10^3 is the unit conversion factor that converts mg/g into mg/mg.

The area-integrated average annual atmospheric particulate phase depositional fluxes in Gg/year ($1 \text{ Gg} = 10^{12} \text{ mg}$) to BS can then be calculated. For simplicity, we give PM as an example:

$$F_{PM}^A = \sum_{i=\text{summer}}^{\text{spring}} \left[\overline{f_{PM_i}^A} \times T_i \times (7.7 \times 10^{10}) \right] / 10^{12} \quad (4)$$

where *i* represents summer, autumn, and winter in 2014, and spring in 2015. The $\overline{f_{PM_i}^A}$ is the average daily atmospheric particulate phase depositional flux of PM ($\text{mg} \cdot \text{m}^{-2} \cdot \text{day}^{-1}$) in *i* season for all sampling sites. T_i is the number of days for *i* season. The expression 7.7×10^{10} is the area of BS (m^2). The 10^{12} is the unit conversion factor that converts mg/year into Gg/year.

2.3.1.2. Atmospheric Dissolved Phase Depositional Fluxes

The daily atmospheric DOC depositional flux ($\text{mg} \cdot \text{m}^{-2} \cdot \text{day}^{-1}$) in *i* season at each sampling site is calculated by equation (5):

$$f_{DOC_i}^A = (C_{DOC_i}^A \times V_i) / (A^* \times t_i) \quad (5)$$

where $C_{DOC_i}^A$ is the mass concentration of DOC (mg/L) in *i* season at each sampling site. V_i is the volume of dissolved phase (L) collected during t_i sampling duration. A^* is the area (m^2) of the cylindrical polyethylene plastic tube receiving dissolved phase deposition samples.

The area-integrated average annual atmospheric DOC depositional flux (F_{DOC}^A) in Gg/year to BS can be calculated by equation (6):

$$F_{DOC}^A = \sum_{i=\text{summer}}^{\text{spring}} \left[\overline{f_{DOC_i}^A} \times T_i \times (7.7 \times 10^{10}) \right] / 10^{12} \quad (6)$$

where $\overline{f_{DOC_i}^A}$ is the average daily atmospheric DOC depositional flux ($\text{mg} \cdot \text{m}^{-2} \cdot \text{day}^{-1}$) in *i* season for all sampling sites.

For atmospheric deposition of DBC (F_{DBC}^A Gg/year), we assumed that the ratio of DBC/DOC in our atmospheric dissolved phase was the same as that measured in the adjacent Yellow Sea (Bao et al., 2017). The area-integrated average annual atmospheric DBC depositional flux into BS can be estimated from our calculated DOC depositional flux and this assumed DBC/DOC ratio.

2.3.2. Riverine Export Fluxes

Due to the inaccessible hydrological database for each river with the exception of the Yellow River, but with the available data on total riverine water discharges into the sea from the adjacent provinces/municipality, the annual riverine export fluxes of TSS (F_{TSS}^R), POC (F_{POC}^R), PBC (F_{PBC}^R), DOC (F_{DOC}^R), and DBC (F_{DBC}^R) in Gg/year to BS can be calculated by the following method. For convenience, we take TSS as an example.

$$F_{TSS}^R = \left[\left(\overline{C_{TSS_{\text{YR}}}^R} \times Q_{\text{YR}} \right) + \sum_{j=\text{Liaoning}}^{\text{Shandong}} \left(\overline{C_{TSS_j}^R} \times Q_j \right) \right] / 10^9 \quad (7)$$

Table 1

Seasonal and Annual Ranges and Averages of Atmospheric PM, POC, PBC, and DOC Concentrations and Daily Depositional Fluxes in Bohai Rim

Sampling period	Season	POC (mg/g)		PBC (mg/g)		DOC (mg/L)		PBC/POC (%)	
		Range	Ave ± SD ^a	Range	Ave ± SD	Range	Ave ± SD	Range	Ave ± SD
Jun 2014 to Aug 2014	Summer	73.7–629.1	334.4 ± 142.6	22.6–181.8	78.8 ± 40.8	0.0–1.8	0.9 ± 0.5	11.5–30.7	24.2 ± 5.9
Sep 2014 to Nov 2014	Autumn	71.0–579.0	285.8 ± 121.5	12.9–87.5	44.7 ± 25.8	0.0–20.9	1.5 ± 1.8 ^b	5.3–32.9	16.4 ± 7.9
Dec 2014 to Feb 2015	Winter	144.1–327.2	253.9 ± 49.9	15.8–90.1	45.3 ± 22.2	0.0–10.7	3.3 ± 3.4	7.0–27.5	17.7 ± 6.9
Mar 2015 to May 2015	Spring	115.9–286.5	182.1 ± 41.2	18.9–51.4	34.0 ± 11.9	0.0–1.7	0.8 ± 0.4	10.9–24.2	18.5 ± 4.2
Jun 2014 to May 2015	Annual	71.0–629.1	260.7 ± 112.8	12.9–181.8	49.8 ± 31.4	0.0–20.9	1.6 ± 2.2 ^b	5.3–32.9	19.1 ± 7.0

Sampling period	Season	PM (mg · m ⁻² · day ⁻¹)		POC (mg · m ⁻² · day ⁻¹)		PBC (mg · m ⁻² · day ⁻¹)		DOC (mg · m ⁻² · day ⁻¹)	
		Range	Ave ± SD	Range	Ave ± SD	Range	Ave ± SD	Range	Ave ± SD
Jun 2014 to Aug 2014	Summer	6.7–52.4	32.2 ± 15.2	2.4–17.3	9.4 ± 4.2	0.5–4.8	2.3 ± 1.3	0.0–3.4	1.8 ± 1.0
Sep 2014 to Nov 2014	Autumn	4.0–57.7	32.3 ± 16.2	1.3–20.7	8.8 ± 5.6	0.3–3.4	1.3 ± 1.0	0.0–24.2	1.5 ± 1.8 ^a
Dec 2014 to Feb 2015	Winter	25.3–112.4	51.1 ± 25.4	6.7–25.5	12.8 ± 6.6	0.7–6.2	2.2 ± 1.5	0.0–1.7	0.5 ± 0.5
Mar 2015 to May 2015	Spring	59.2–188.1	106.8 ± 35.9	9.1–40.3	19.5 ± 8.2	1.5–9.0	3.8 ± 2.2	0.0–1.9	0.9 ± 0.7
Jun 2014 to May 2015	Annual	4.0–188.1	57.4 ± 40.4	1.3–40.3	12.9 ± 7.8	0.3–9.0	2.4 ± 1.8	0.0–24.2	1.2 ± 1.2 ^a

Note. PM = particulate matter; POC = particulate organic carbon; PBC = particulate black carbon; DOC = dissolved organic carbon.

^aAve ± SD denotes average ± standard deviation. ^bThe two overwhelmingly high DOC values were not involved in the calculations of average DOC concentrations and daily depositional fluxes.

where j consists of Liaoning, Hebei, Tianjin, and Shandong provinces/municipality (Figure 1a). $\overline{C_{TSS_{YR}}^R}$ and $\overline{C_{TSS_j}^R}$ each represents the measured mean annual TSS concentrations (mg/L) from the Yellow River and other rivers that enter into the sea from j provinces/municipality. Q_{YR} and Q_j are the annual water discharges (m³/year) of the Yellow River and other rivers that enter into the BS from j provinces/municipality, respectively. The 10⁹ is the unit conversion factor that converts g/year into Gg/year.

2.3.3. Exchange Fluxes in Bohai Strait

The import fluxes (Gg/year) from NYS to BS and export fluxes (Gg/year) from BS to NYS are calculated through multiplying the mean annual concentrations (mg/L) measured at sites east of the northern Bohai Strait and at sites west of the southern Bohai Strait (Figure 1b) by their corresponding water import flux (Q_{im} , m³/year) and export flux (Q_{ex} , m³/year). The following gives the calculation formula of TSS:

$$F_{TSS_{im}}^S = \left(\overline{C_{TSS_{im}}^S} \times Q_{im} \right) / 10^9 \quad (8)$$

$$F_{TSS_{ex}}^S = \left(\overline{C_{TSS_{ex}}^S} \times Q_{ex} \right) / 10^9 \quad (9)$$

2.3.4. Sedimentary Sink Fluxes

The calculations of the sedimentary sink fluxes in BS were elaborated in our recent work based on the high-density sediment sampling (Figure 1b; Fang et al., 2015). According to the calculations, 913 ± 219 Gg/year and 157 ± 41 Gg/year of POC and PBC were sequestered in BS sediments, respectively.

3. Results

3.1. Atmospheric PM, POC, PBC, and DOC Concentrations and Depositional Fluxes

The atmospheric PM, POC, PBC, and DOC concentrations, and daily depositional fluxes at 12 coastal sites in each season are plotted in Figures S1 and 2, respectively, while Table 1 summarizes seasonal and annual ranges and averages for all sites. The POC and PBC concentrations during the 1-year sampling period ranged from 71.0 to 629.1 and 12.9 to 181.8 mg/g, and averaged 260.7 ± 112.8 and 49.8 ± 31.4 mg/g, respectively. PBC constituted a significant fraction of POC, with an annual average PBC/POC of 19.1 ± 7.0% (range: 5.3%–32.9%). The seasonal average concentrations of POC and PBC both decreased in the order of summer > autumn ≈ winter > spring (Table 1), with spring averages amounting to only 54% and 43% of those in summertime, respectively. The POC and PBC concentrations had similar spatial distributions (Figures S1a and S1b), with the lowest levels occurring at DY and RC, where levels were approximately 2–3 times lower than those at other sites; both sites are characterized by relatively sparse industrial activities. In contrast,

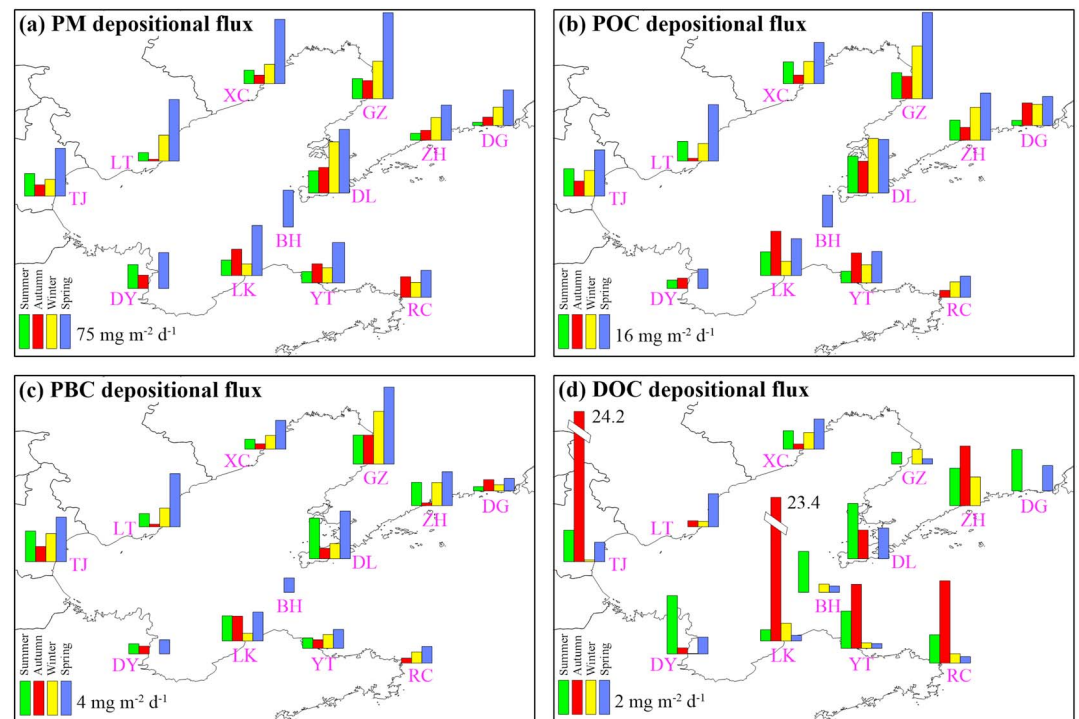


Figure 2. Temporal and spatial distributions of atmospheric (a) particulate matter (PM), (b) particulate organic carbon (POC), (c) particulate black carbon (PBC), and (d) dissolved organic carbon (DOC) daily depositional fluxes in Bohai Rim.

the DOC concentrations showed distinct seasonal patterns (Figure S1c and Table 1), with the highest values in winter (3.3 ± 3.4 mg/L) and autumn (1.5 ± 1.8 mg/L) and the lowest levels in spring (0.8 ± 0.4 mg/L) and summer (0.9 ± 0.5 mg/L). In addition, some overwhelmingly high outliers were observed, such as 20.9 mg/L at TJ and 19.6 mg/L at LK in autumn (Figure S1c and Table S1). The spatial variation was more pronounced in DOC concentrations than in those of POC and PBC, as reflected by the larger RSD in seasonal average DOC concentrations (52%–123%) than in those of POC (20%–43%) and PBC (35%–58%).

The atmospheric PM daily depositional fluxes during the sampling period varied by up to a factor of 47, ranging from 4.0 to $188.1 \text{ mg} \cdot \text{m}^{-2} \cdot \text{day}^{-1}$ and averaging $57.4 \pm 40.4 \text{ mg} \cdot \text{m}^{-2} \cdot \text{day}^{-1}$ (Table 1). The highest PM daily depositional flux (average: $106.8 \pm 35.9 \text{ mg} \cdot \text{m}^{-2} \cdot \text{day}^{-1}$) was observed in spring, which was on average ~ 2 – 3 times higher than that in other seasons (32.2 – $51.1 \text{ mg} \cdot \text{m}^{-2} \cdot \text{day}^{-1}$). With respect to the spatial patterns, values were high at DL and GZ (annual averages: $\sim 90 \text{ mg} \cdot \text{m}^{-2} \cdot \text{day}^{-1}$) than at the other sites (average: 36 – $58 \text{ mg} \cdot \text{m}^{-2} \cdot \text{day}^{-1}$) (Figure 2a and Table S1). The POC and PBC daily depositional fluxes also displayed large variations and varied by factors of 31 and 30, ranging from 1.3 to 40.3 and 0.3 to $9.0 \text{ mg} \cdot \text{m}^{-2} \cdot \text{day}^{-1}$, and averaging 12.9 ± 7.8 and $2.4 \pm 1.8 \text{ mg} \cdot \text{m}^{-2} \cdot \text{day}^{-1}$, respectively. Of particular note was that the temporal and spatial trends between POC, PBC, and PM daily depositional fluxes were very consistent (Figures 2a–2c), as clearly evidenced by the significant positive correlations among them (Figure S2), indicating that PM was the carrier of POC and PBC to BS. In contrast, the DOC daily depositional flux displayed almost the opposite temporal trend (Figure 2d) to those of PM, POC, and PBC, with summer and autumn averages (1.5 – $1.8 \text{ mg} \cdot \text{m}^{-2} \cdot \text{day}^{-1}$) that were 2–3 times higher than those in winter and spring (0.5 – $0.9 \text{ mg} \cdot \text{m}^{-2} \cdot \text{day}^{-1}$; Table 1).

The area-integrated atmospheric PM, POC, PBC, and DOC depositional fluxes to BS were $1,564 \pm 347$, 355 ± 89 , 68 ± 22 , and 33 ± 15 Gg/year, respectively (Figure 3a). Spring contributed almost half of the total deposition of PM, POC, and PBC, with the other three seasons contributing the remaining half (Figure 3b). However, the seasonal contributions of DOC (Figure 3b) differed significantly from those of the particulate phases, with summer, autumn, and winter contributing over 80% of the total deposition and spring accounting for the remaining amount. Summing POC and DOC indicated that 388 ± 90 Gg of atmospheric OC was deposited into the BS annually, of which more than 90% was in the particulate phase.

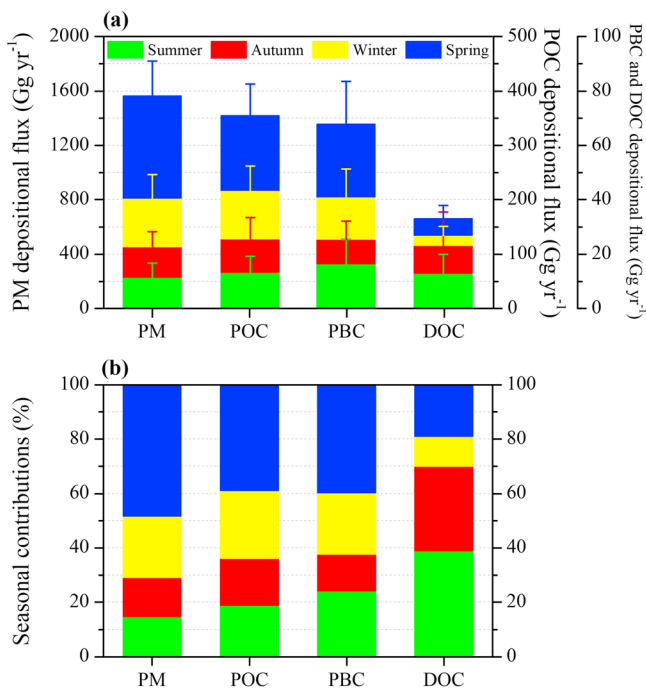


Figure 3. (a) Area-integrated atmospheric particulate matter (PM), particulate organic carbon (POC), particulate black carbon (PBC), and dissolved organic carbon (DOC) depositional fluxes to the Bohai Sea, and (b) their seasonal contributions.

3.2. Riverine TSS, POC, PBC, DOC, and DBC Concentrations and Export Fluxes

Riverine TSS, POC, and PBC concentrations during the four sampling periods varied by more than 2 orders of magnitude, with ranges of 1.54–2,000.00, 0.14–28.50, and 0.01–5.72 mg/L, and averaging 72.29 ± 212.25 , 3.81 ± 3.89 , and 0.37 ± 0.67 mg/L, respectively (Table S2). PBC in riverine water samples accounted for 2.2%–35.4% of POC, with an average PBC/POC ratio of $9.0 \pm 4.3\%$. This was only half the value in atmospheric deposition samples, indicating different sources of POC and PBC in the two matrices. The largest TSS, POC, and PBC concentrations were observed in concurrent samples from the Yellow River during August 2013 sampling campaign (Table S2); values were 12–27 times higher than those obtained in August 2014. As with the particulate phases of atmospheric deposition samples, the temporal and spatial patterns of riverine TSS, POC, and PBC were very consistent (Figures 4a–4c, 4f–4h, and 4k–4m), with the temporally highest levels in August 2013 and the spatially highest levels in Bohai Bay. The riverine TSS, POC, and PBC concentrations were significantly correlated (Figures S3a and S3b).

Concentrations of riverine DOC and DBC varied from 2.92 to 149.78 mg/L (average: 38.72 ± 37.96 mg/L) and from 0.09 to 1.33 mg/L (average: 0.37 ± 0.21 mg/L), respectively (Table S2). DBC comprised 0.1%–9.5% of DOC (average: $1.9 \pm 1.8\%$). The temporal and spatial patterns of DOC and DBC concentrations were similar (Figures 5d, 5e, 5i, 5j, 5n, and 5o), with the temporally highest levels in October 2014 and the spatially highest levels in Bohai Bay. The correlation between DOC and DBC concentrations was significant (Figure S3c), but there was no correlation between the particulate and dissolved phases (Figure S3d).

Based on the hydrological data sets and the measured concentrations, it was estimated that 781.9, 150.4, 924.7, and 16.3 Gg/year of POC, PBC, DOC, and DBC were exported from rivers to BS during 2013 and 67.5, 5.8, 1,118.0, and 6.4 Gg/year were exported during 2014, respectively. The export of OC and BC displayed strong interannual variations, which were more pronounced for the particulate phases (varying by over 1 order of magnitude) than for the dissolved phases (varying by less than 3 times). The Yellow River alone contributed 86%, 90%, 31%, and 37% of total annual POC, PBC, DOC, and DBC exports during 2013, and 39%, 40%, 51%, and 32% during 2014, respectively.

3.3. TSS, POC, PBC, DOC, and DBC Concentrations and Exchange Fluxes in the Bohai Strait

The TSS and carbonaceous concentrations were significantly lower in the Bohai Strait samples than in riverine water samples (Tables S2 and S3) and exhibited two major characteristics (Figure 5). One was a higher seasonal concentration in spring and winter than in summer and autumn, which was more pronounced for the particulate phases measured at sites west of the southern Bohai Strait (Figures 5a–5c). The other was the geographically higher concentrations for sites west of the southern Bohai Strait (annual average TSS, POC, PBC, DOC, and DBC concentrations were 10.17 ± 7.98 , 0.223 ± 0.074 , 0.021 ± 0.009 , 10.44 ± 3.55 , and 0.079 ± 0.005 mg/L, respectively) than for sites east of the northern Bohai Strait (2.40 ± 0.65 , 0.100 ± 0.015 , 0.007 ± 0.003 , 9.83 ± 3.48 , and 0.051 ± 0.003 mg/L, respectively). The calculated export fluxes of TSS, POC, PBC, DOC, and DBC from BS to NYS through the southern Bohai Strait were $16,266 \pm 12,776$, 357 ± 118 , 33 ± 15 , $16,704 \pm 5,684$, and 126 ± 8 Gg/year, and the import fluxes from NYS to BS through the northern Bohai Strait were $3,836 \pm 1,034$, 159 ± 24 , 12 ± 4 , $15,728 \pm 5,564$, and 81 ± 6 Gg/year, respectively.

4. Discussion

4.1. Atmospheric PM, POC, and PBC Deposition to BS: Impact of Spring Dust Storm Events

Dust storms are a typical natural weather event in northern China in spring (March–May). During the spring 2015 atmospheric deposition sampling campaign, China's National Weather Bureau recorded two major dust

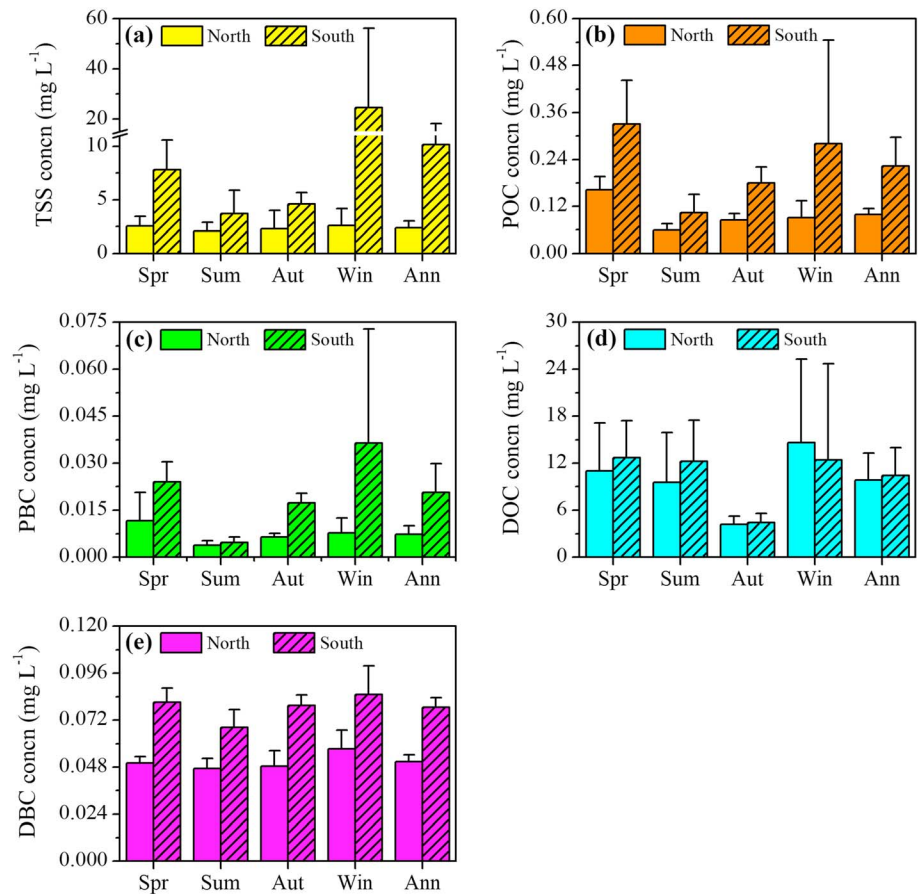


Figure 5. Seasonal and annual average (a) TSS, (b) POC, (c) PBC, (d) DOC, and (e) DBC concentrations in the northern and southern Bohai Strait. Abbreviations for concn in vertical axis and for Spr, Sum, Aut, Win, and Ann in horizontal axis are concentration, spring, summer, autumn, winter, and annual, respectively.

(expressed as mgC/g soil) (Yang et al., 2010). Consequently, the springtime deposition samples affected by the strong dust storms had the lowest seasonal average POC and PBC concentrations (POC: 182.1 mg/g; PBC: 34.0 mg/g). Concentrations were higher in other seasons that were either little affected or unaffected by dust storms (POC: 253.9–334.4 mg/g; PBC: 44.7–78.8 mg/g; Table 1). When taking the overwhelmingly high loadings of dust particle deposition in spring into account (spring: $106.8 \text{ mg} \cdot \text{m}^{-2} \cdot \text{day}^{-1}$; others: $32.2\text{--}51.1 \text{ mg} \cdot \text{m}^{-2} \cdot \text{day}^{-1}$), the seasonal patterns of POC and PBC daily depositional fluxes were completely opposite to those of their concentrations, with spring POC and PBC daily depositional fluxes (19.5 and $3.8 \text{ mg} \cdot \text{m}^{-2} \cdot \text{day}^{-1}$) significantly larger than those observed in other seasons ($8.8\text{--}12.8$ and $1.3\text{--}2.3 \text{ mg} \cdot \text{m}^{-2} \cdot \text{day}^{-1}$; Table 1). This in turn resulted in the highest area-integrated POC and PBC depositional fluxes in spring (138 and 27 Gg), which were 1.6–2.2 and 1.7–3.0 times higher than those in other seasons (62–89 and 9–16 Gg), respectively (Figure 3a).

To estimate the net effect of dust storm events on PM, POC, and PBC deposition to the BS quantitatively, we assumed that their daily depositional fluxes in spring, if not influenced by dust storms, were of similar levels to those in other seasons. It was then calculated that the 6 days of dust storms in spring 2015, which accounted for only 6.5% of spring days (92 days), were responsible for up to half of the total spring PM (64%), POC (48%), and PBC (50%) deposition to the BS. Despite this rough estimation, it explicitly demonstrated the strong impact of this type of natural weather event (i.e., natural perturbation) on BS carbon cycling.

4.2. Riverine OC and BC Concentrations: Impact of Anthropogenic Activity

The dense network of riverine water sampling in Bohai Rim in this study provided us with a good opportunity to identify the close affinity between regional anthropogenic activity and terrestrial riverine OC and BC

concentrations. The regions adjacent to the BS, consisting of Liaoning Province in Liaodong Bay (LDB), Beijing and Tianjin municipalities in Bohai Bay (BHB), and Shandong Province in Laizhou Bay (LZB, Figure 1), differ significantly in their population densities and economic development indexes (Figure S4). Beijing and Tianjin municipalities are the most developed industrial and commercial megacities in Bohai Rim, with the highest levels of anthropogenic activity. The gross domestic product (GDP) per capita is ~1.5 times higher in Beijing and Tianjin than in Liaoning and Shandong (Figure S4), which correlates well with the observed higher riverine OC and BC concentrations of both particulate and dissolved phases in BHB compared with those in LDB and LZB, as shown in Figures 4l–4o. It can therefore be concluded that regional anthropogenic activity in Bohai Rim has a significant impact on the watershed riverine OC and BC concentrations. The varying concentration distributions in environmental compartments in response to the differences in intensity of regional anthropogenic activity were also reflected in the sedimentary concentrations of BC in riverine sediments and those of some other anthropogenic pollutants (e.g., polycyclic aromatic hydrocarbons (PAHs) and heavy metals) in riverine/sea waters, sediments, and even organisms (Fang et al., 2014; Gao et al., 2014; Jiang et al., 2010; Zhang et al., 2009). Our recent studies have found higher BC concentrations in BHB river sediments (chemical thermal oxidation, CTO-375) than in those from LZB (thermal optical reflectance, TOR; Fang et al., 2014; Jiang et al., 2010), despite the methodological ring trial-detected BC values using the CTO-375 method that were 2–7 times lower than those detected using the TOR method in terms of the sediment matrix (Hammes et al., 2007; Han et al., 2011).

4.3. TSS, POC, and PBC Seasonal Concentration Patterns in Southern Bohai Strait: Combined Impact of East Asian Monsoon and Hydrodynamic Conditions

Although the TSS, POC, and PBC concentrations measured in this study in the southern Bohai Strait show significant discrepancies in comparison to those in previous studies (Bi et al., 2011; Yang et al., 2011), the relative magnitudes of the seasonal concentration patterns are generally consistent. They are all with higher values in winter and spring and lower levels in the other seasons (Figures 5a–5c). The combined impact of the prevailing East Asian monsoon in winter and spring and the regionally specific hydrodynamic conditions may account for most of the seasonal variations.

As a typical continental shelf marginal sea, the BS is significantly affected by terrestrial inputs from rivers. The Yellow River was of particular interest in this study, because it is the world's second largest river in terms of sediment load, and its sediment export has a dramatic impact on the BS ecosystem. It is estimated that more than 80% of Yellow River sediment discharges into the BS in summer (Bi et al., 2011; Fang et al., 2016). During this period, the water column in LZB is highly stratified and vertical mixing is remarkably weakened. This leads to rapid deposition of riverine sediments within the nearshore areas of the Yellow River mouth (<30 km), even during the "Water and Sediment Regulation" period, when ~30% of the annual sediment is delivered into the sea (Bi et al., 2011). This implies that there are no large amounts of sediments passing through the southern Bohai Strait during summer, resulting in relatively low TSS, POC, and PBC concentrations in summertime. During winter and spring, however, the strong northerly and northwesterly East Asian monsoon prevails, generating waves as high as 7 m that propagate toward the coast of the Yellow River delta (Bi et al., 2011). These large waves give rise to intensive resuspension of the estuarine seabed sediments off the Yellow River delta due to the elevated bottom shear stress (Yang et al., 2011). Moreover, intense vertical mixing maintains the sediments in suspension, making it much easier for their transport and subsequent export. Driven by the eastward coastal currents (Figure 1b) induced by the prevailing northerly and northwesterly winds, the resuspended sediments are transported southward to LZB and then transported eastward along the coast of Shandong Peninsula to the NYS through the southern Bohai Strait (Bi et al., 2011). As a result, the TSS, POC, and PBC concentrations are higher during winter and spring than in other seasons, especially summertime. A similar seasonal pattern of TSS in the southern Bohai Strait has been reported by Bi et al. (2011), who developed an exponential empirical model to retrieve TSS concentrations from accessible Moderate Resolution Imaging Spectroradiometer imagery data.

The East Asian monsoon and associated hydrodynamic conditions also plays an important role in sorting sedimentary BC from various combustion sources with distinct physical properties (especially particle size), as reported in our recent study (Fang et al., 2016). In that study, we found that within 5–30 km away from the Yellow River estuary, the fossil fuel combustion-derived BC increased exponentially from 10% to 80%,

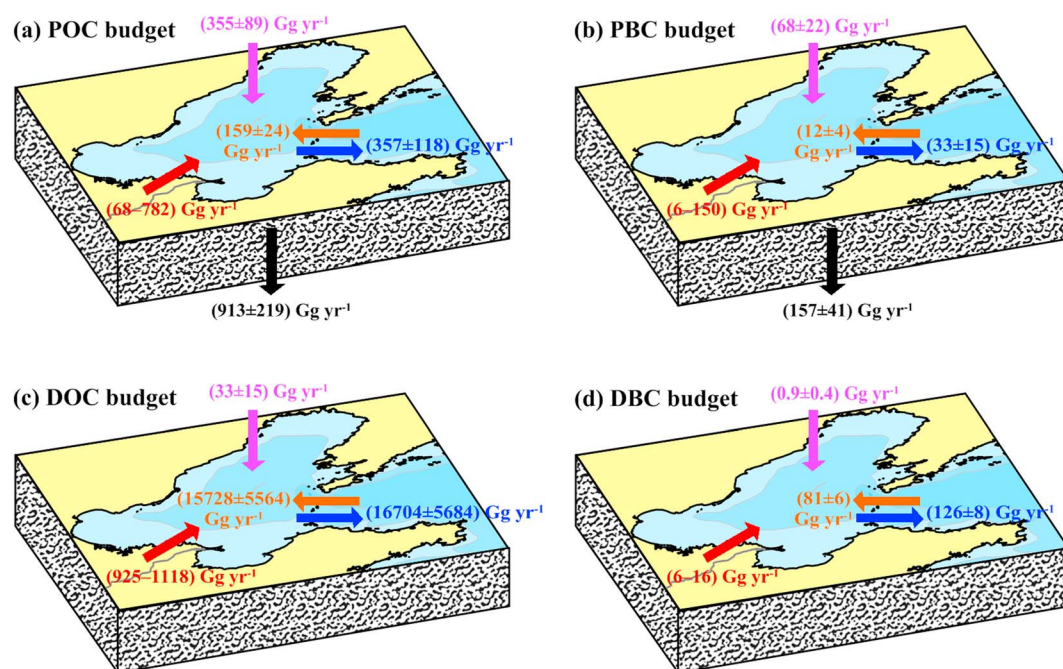


Figure 6. The (a) POC, (b) PBC, (c) DOC, and (d) DBC budgets in coastal Bohai Sea. Purple, red, orange, blue, and black arrows denote processes of atmospheric deposition, riverine discharge, import from NYS to BS, export from BS to NYS, and sequestration to sediments, respectively.

and the biomass burning-derived BC accordingly declined exponentially from 90% to 20%. Beyond ~30 km, however, they both changed slightly due to the significantly weakened hydrodynamic conditions.

4.4. POC, PBC, DOC, and DBC Budgets in Coastal BS

The calculated POC, PBC, DOC, and DBC budgets in coastal semienclosed BS are illustrated in Figure 6. The calculations included only the major exogenous cycling processes that we studied (i.e., atmospheric and riverine delivery, exchange in the Bohai Strait, and sedimentation); the internal cycling processes (mainly marine primary production and respiration) were not involved. In general, the budgets and therefore source-to-sink processes can be broadly classified into two categories. The budgets for each individual particulate phase (i.e., POC versus PBC) or dissolved phase (i.e., DOC versus DBC) displayed similar patterns, but there were distinct differences between the particulate and dissolved phases.

For POC and PBC, the budgets were to some extent balanced (Figures 6a and 6b). Atmospheric deposition and riverine discharge were of similar importance, with these two input pathways accounting for on average >80% of the total exogenous influx. The input from NYS to the northern Bohai Strait contributes the remaining <20%. As a semienclosed marginal sea strongly affected by an abundance of riverine inputs (especially from the Yellow River), the somewhat unexpected higher proportion of POC and PBC from atmospheric deposition indicates the strong impact of a natural weather event, that is, dust storms, on the BS ecosystem.

Sinking and subsequent sequestration to sediments dominated POC and PBC removal, accounting for ~70% of total output. The semienclosed (resulting in weak water exchange) and shallow (mean water depth of 18 m) characteristics of BS are likely responsible for such high POC and PBC sequestration potential in BS sediments. In addition to sedimentation, export to NYS through the southern Bohai Strait was also an important transport pathway, accounting for up to ~30% of total output. The net POC and PBC exchanges in the Bohai Strait both exhibited net export from BS to NYS, which was in agreement with the net particle transport through the Bohai Strait obtained by a grain size trend analysis (Cheng et al., 2004; Hu et al., 2011). Hence, the BS can be considered an important source of suspended particles, POC, and PBC for the NYS.

In contrast, however, the DOC and DBC budgets in BS (Figures 6c and 6d) differed dramatically from those of POC and PBC in several aspects, including import, export, and exchange processes. The inputs of both DOC

and DBC to BS were predominantly (>83%) from NYS through the water inflow in the northern Bohai Strait, with riverine discharge and atmospheric deposition together accounting for <20% of total influx. The water outflow to NYS through the southern Bohai Strait can be regarded as the exclusive export route for DOC and DBC, although a minor fraction may be adsorbed onto sinking particles that subsequently settle and are finally sequestered in sediments (Coppola et al., 2014; Fang et al., 2017). The dominant import and export pathways for both DOC and DBC in the Bohai Strait result in an exchange that is in a state of relative dynamic equilibrium. This situation is particularly true for DOC, because the net exchange flux of DOC accounted for only 5.8% of the export flux from BS to NYS).

Several studies on BC (including PBC and DBC) cycling and budgets have been conducted regionally and globally. Regional observational studies of PBC have focused on geographically separated areas, such as the New England continental shelf (Gustafsson & Gschwend, 1998), the Gulf of Maine (Flores-Cervantes et al., 2009), the Northern European shelf (Sánchez-García et al., 2012), and the inner shelf of the East China Sea (L. Huang et al., 2016). These studies identified different PBC input patterns (e.g., the relative magnitudes of atmospheric deposition and riverine discharge differed), but they all concluded that coastal sediment is an important sink of PBC from active cycling in the global biogeosphere, which agrees well with the present study. Globally, coastal sediment has been estimated to account for 90% of global PBC burial, despite the fact that coastal areas account for only 10% of the area of the world's ocean (Fang et al., 2015). Most studies of DBC have determined its concentration and flux in river and seawater samples (Dittmar, 2008; Dittmar et al., 2012; Jaffé et al., 2013), but little attention has been paid on its levels in the atmosphere. Rough estimates have indicated that the global riverine discharge and atmospheric deposition of DBC to the ocean are 27 and 1.8 Tg/year, respectively (Bao et al., 2017; Jaffé et al., 2013), with a ratio of riverine to atmospheric delivery of 15. The ratio of riverine to atmospheric delivery in coastal BS ranged from 7 to 18, which corresponds well with the global average level. This implies that the coastal BS may serve as an ideal specimen for studying global DBC source-to-sink processes. In addition, regional (e.g., this study) and global databases both demonstrate that future studies should calculate PBC and DBC fluxes independently, which will elucidate regional and global BC source-to-sink processes and some other associated biogeochemical implications.

4.5. Uncertainties in Budget Calculations

There were some uncertainties associated with the POC, PBC, DOC, and DBC budget calculations for the BS. The uncertainties originated mainly from the different time scales integrated in each environmental compartment and a lack of consideration of other biogeochemical processes. As regards the time scales, the fluxes of atmospheric and riverine delivery reflected imports from the sampling year(s), but the sedimentary (surface 0–3 cm) sink flux in BS in this study reflected the mean sequestration level over recent decades because of the relatively low sedimentation rates in BS (0.1–0.4 cm/year; Qin et al., 2011). Available studies have explicitly demonstrated the remarkable interannual variations and fluctuations in the atmospheric emissions (Cao et al., 2006; R. Wang et al., 2012) and riverine exports (Cauwet & Mackenzie, 1993; X. Wang et al., 2012, 2016; Zhang et al., 1992) in Bohai Rim. In a case study of the Yellow River, export fluxes during 1987–2015 (approximately corresponding to the time covered by the sediment samples in this study) were calculated to range from 27 to 6,100 Gg/year for POC and from 31 to 572 Gg/year for DOC, both of which varied by more than 1 order of magnitude. As regards the processes, other possible sources, such as in situ coastal primary production (but not for pyrogenic PBC and DBC), coastal tidal wetlands, benthic resuspension, and submarine groundwater discharge, were not included. Similarly, other possible removal mechanisms, such as in situ respiration, sorption onto sinking particles, salinity-induced flocculation, mineralization, photochemical oxidation, and microbial degradation, were also not included (Bauer et al., 2013; Dai et al., 2012; Ding et al., 2014; Fang et al., 2017). It was estimated that primary production may contribute ~39,000 Gg/year of OC to BS, of which ~78% may be consumed by respiration. This implies that the unconsidered internal cycling processes of primary production and respiration also have significant influences on BS carbon budgets. Additionally, in terms of BC, the quantification methods applied also affected the determination of BC concentration and therefore budget construction (Hammes et al., 2007). A methodological ring trial revealed that BC concentrations detected by BPCA method were significantly lower than those detected by TOR method, with the former quantifying the highly condensed aromatic ring structures and the latter quantifying nearly the whole BC continuum, ranging from micron-sized char (1–100 μm) to submicron-sized soot particles (<1 μm) (Hammes et al., 2007; Han et al., 2011). All of these considerations imply that continuous field

observational studies, more details of the biogeochemical processes involved, and consistent BC quantification methods are urgently needed to elucidate OC and BC budget construction.

5. Conclusions

In this study, the cycling and budgets of POC, PBC, DOC, and DBC in coastal semienclosed BS were investigated based on the multimedial sampling campaigns that included sampling of atmospheric deposition, river water, seawater, and sediments, together with simultaneous quantification of both particulate and dissolved OC and BC. The major conclusions were as follows.

1. Almost half of the annual total PM, POC, and PBC deposition to BS occurred in spring, when dust storms had a strong impact; 6 days of spring dust storms accounted for up to half of the spring total PM, POC, and PBC deposition.
2. The spatial patterns of POC, PBC, DOC, and DBC concentrations in riverine water samples in Bohai Rim correlated significantly with regional differences in anthropogenic activity, with relatively high levels in BHB and relatively low levels in LDB and LZB.
3. The combination of the East Asian monsoon and associated hydrodynamic conditions resulted in seasonal patterns of TSS, POC, and PBC concentration in the southern Bohai Strait, with higher values in winter and spring and lower values in the other two seasons.
4. The cycling and budgets for each individual particulate phase (i.e., POC versus PBC) or dissolved phase (i.e., DOC versus DBC) in coastal BS displayed similar patterns, but there were some distinct differences between the particulate and dissolved phases. Atmospheric and riverine delivery dominated the input of the particulate phases (>80%), sequestration to sediments dominated their removal (~70%), and exchanges in the Bohai Strait resulted in net export from BS to NYS. Exchanges in the Bohai Strait dominated both the import and export pathways of the dissolved phases, which were therefore considered to be in a relatively dynamic equilibrium. The substantially different time scales integrated in each environmental compartment, a lack of consideration of some other biogeochemical processes, and the inconsistent BC quantification methods resulted in some uncertainties in these budget calculations.

Acknowledgments

The data for this paper are available in supporting information Tables S1–S3. This work was financially supported by National Natural Scientific Foundation of China (41703087, 91744203, 41473091, and 41722603), State Key Laboratory of Organic Geochemistry of GIGCAS (SKLOG-201620), Basic Scientific Fund for National Public Research Institutes of China (2017S01), Key Laboratory of Yangtze River Water Environment of Ministry of Education in Tongji University (YRWEF201802), and Key Laboratory of Coastal Environmental Processes and Ecological Remediation of YICCAS (2016KFJJ04). The authors wish to thank the crew of R/V *Dong Fang Hong 2* of Ocean University of China for collecting the seawater samples within the Bohai Strait. We also thank the Editor (Sara Mikaloff Fletcher) and two anonymous reviewers who provided constructive comments which strengthened the manuscript.

References

- Andersson, A., Deng, J., Du, K., Zheng, M., Yan, C., Skold, M., & Gustafsson, Ö. (2015). Regionally-varying combustion sources of the January 2013 severe haze events over Eastern China. *Environmental Science & Technology*, *49*(4), 2038–2043. <https://doi.org/10.1021/es503855e>
- Bao, H., Niggemann, J., Luo, L., Dittmar, T., & Kao, S. (2017). Aerosols as a source of dissolved black carbon to the ocean. *Nature Communications*, *8*(1), 510–517. <https://doi.org/10.1038/s41467-017-00437-3>
- Bauer, J. E., Cai, W. J., Raymond, P. A., Bianchi, T. S., Hopkinson, C. S., & Regnier, P. A. G. (2013). The changing carbon cycle of the coastal ocean. *Nature*, *504*(7478), 61–70. <https://doi.org/10.1038/nature12857>
- Bi, N., Yang, Z., Wang, H., Fan, D., Sun, X., & Lei, K. (2011). Seasonal variation of suspended-sediment transport through the southern Bohai Strait. *Estuarine, Coastal and Shelf Science*, *93*(3), 239–247. <https://doi.org/10.1016/j.ecss.2011.03.007>
- Bianchi, T. S., Allison, M. A., & Cai, W. J. (2014). *Biogeochemical dynamics at major river-coastal interfaces: Linkages with global change*. New York: Cambridge University Press.
- Bird, M. I., Wynn, J. G., Saiz, G., Wurster, C. M., & McBeath, A. (2015). The pyrogenic carbon cycle. *Annual Review of Earth and Planetary Sciences*, *43*(1), 273–298. <https://doi.org/10.1146/annurev-earth-060614-105038>
- Bond, T. C., Streets, D. G., Yarber, K. F., Nelson, S. M., Woo, J. H., & Klimont, Z. (2004). A technology-based global inventory of black and organic carbon emissions from combustion. *Journal of Geophysical Research*, *109*, D14203. <https://doi.org/10.1029/2003JD003697>
- Brodowski, S., Rodionov, A., Haumaier, L., Glaser, B., & Amelung, W. (2005). Revised black carbon assessment using benzene polycarboxylic acids. *Organic Geochemistry*, *36*(9), 1299–1310. <https://doi.org/10.1016/j.orggeochem.2005.03.011>
- Cao, G., Zhang, X., & Zheng, F. (2006). Inventory of black carbon and organic carbon emissions from China. *Atmospheric Environment*, *40*(34), 6516–6527. <https://doi.org/10.1016/j.atmosenv.2006.05.070>
- Cauwet, G., & Mackenzie, F. T. (1993). Carbon inputs and distribution in estuaries of turbid rivers: The Yang Tze and Yellow Rivers (China). *Marine Chemistry*, *43*(1–4), 235–246. [https://doi.org/10.1016/0304-4203\(93\)90229-H](https://doi.org/10.1016/0304-4203(93)90229-H)
- Chen, L., Zhang, M., Zhu, J., & Skorokhod, A. (2017). Model analysis of soil dust impacts on the boundary layer meteorology and air quality over East Asia in April 2015. *Atmospheric Research*, *187*(Supplement C), 42–56. <https://doi.org/10.1016/j.atmosres.2016.12.008>
- Cheng, P., Gao, S., & Bokuniewicz, H. (2004). Net sediment transport patterns over the Bohai Strait based on grain size trend analysis. *Estuarine, Coastal and Shelf Science*, *60*(2), 203–212. <https://doi.org/10.1016/j.ecss.2003.12.009>
- Cong, Z., Kang, S., Gao, S., Zhang, Y., Li, Q., & Kawamura, K. (2013). Historical trends of atmospheric black carbon on Tibetan Plateau as reconstructed from a 150-year lake sediment record. *Environmental Science & Technology*, *47*(6), 2579–2586. <https://doi.org/10.1021/es3048202>
- Coppola, A. I., Ziolkowski, L. A., Masiello, C. A., & Druffel, E. R. M. (2014). Aged black carbon in marine sediments and sinking particles. *Geophysical Research Letters*, *41*, 2427–2433. <https://doi.org/10.1002/2013GL059068>
- Dai, M., Yin, Z., Meng, F., Liu, Q., & Cai, W. J. (2012). Spatial distribution of riverine DOC inputs to the ocean: An updated global synthesis. *Current Opinion in Environmental Sustainability*, *4*(2), 170–178. <https://doi.org/10.1016/j.cosust.2012.03.003>
- Ding, Y., Cawley, K. M., da Cunha, C. N., & Jaffé, R. (2014). Environmental dynamics of dissolved black carbon in wetlands. *Biogeochemistry*, *119*(1–3), 259–273. <https://doi.org/10.1007/s10533-014-9964-3>

- Dittmar, T. (2008). The molecular level determination of black carbon in marine dissolved organic matter. *Organic Geochemistry*, 39(4), 396–407. <https://doi.org/10.1016/j.orggeochem.2008.01.015>
- Dittmar, T., de Rezende, C. E., Manecki, M., Niggemann, J., Ovalle, A. R. C., Stubbins, A., & Bernardes, M. C. (2012). Continuous flux of dissolved black carbon from a vanished tropical forest biome. *Nature Geoscience*, 5(9), 618–622. <https://doi.org/10.1038/ngeo1541>
- Dutta, T., Kwon, E., Bhattacharya, S. S., Jeon, B. H., Deep, A., Uchimiya, M., & Kim, K.-H. (2017). Polycyclic aromatic hydrocarbons and volatile organic compounds in biochar and biochar-amended soil: A review. *Global Change Biology. Bioenergy*, 9(6), 990–1004. <https://doi.org/10.1111/gcbb.12363>
- Fang, Y., Chen, Y., Lin, T., Pan, X., Tian, C., Tang, J., et al. (2014). Distribution of black carbon and its correlation with persistent organic pollutants (POPs) in the surface sediments of coastal zone, Laizhou Bay (in Chinese). *Geochimica*, 43(4), 329–337.
- Fang, Y., Chen, Y., Tian, C., Lin, T., Hu, L., Huang, G., et al. (2015). Flux and budget of BC in the continental shelf seas adjacent to Chinese high BC emission source regions. *Global Biogeochemical Cycles*, 29, 957–972. <https://doi.org/10.1002/2014GB004985>
- Fang, Y., Chen, Y., Tian, C., Lin, T., Hu, L., Li, J., & Zhang, G. (2016). Application of PMF receptor model merging with PAHs signatures for source apportionment of black carbon in the continental shelf surface sediments of the Bohai and yellow seas, China. *Journal of Geophysical Research: Oceans*, 121, 1346–1359. <https://doi.org/10.1002/2015JC011214>
- Fang, Z., Yang, W., Chen, M., & Ma, H. (2017). Source and fate of dissolved black carbon in the western South China Sea during the southwest monsoon prevailing season. *Journal of Geophysical Research: Biogeosciences*, 122, 2817–2830. <https://doi.org/10.1002/2017JG004014>
- Flores-Cervantes, D. X., Plata, D. L., MacFarlane, J. K., Reddy, C. M., & Gschwend, P. M. (2009). Black carbon in marine particulate organic carbon: Inputs and cycling of highly recalcitrant organic carbon in the Gulf of Maine. *Marine Chemistry*, 113(3–4), 172–181. <https://doi.org/10.1016/j.marchem.2009.01.012>
- Gao, X., Zhou, F., & Chen, C.-T. A. (2014). Pollution status of the Bohai Sea: An overview of the environmental quality assessment related trace metals. *Environment International*, 62, 12–30. <https://doi.org/10.1016/j.envint.2013.09.019>
- Guo, L., Semiletov, I., Gustafsson, Ö., Ingri, J., Andersson, P., Dudarev, O., & White, D. (2004). Characterization of Siberian Arctic coastal sediments: Implications for terrestrial organic carbon export. *Global Biogeochemical Cycles*, 18, GB1036. <https://doi.org/10.1029/2003GB002087>
- Gustafsson, Ö., & Gschwend, P. M. (1998). The flux of black carbon to surface sediments on the New England continental shelf. *Geochimica et Cosmochimica Acta*, 62(3), 465–472. [https://doi.org/10.1016/S0016-7037\(97\)00370-0](https://doi.org/10.1016/S0016-7037(97)00370-0)
- Hammes, K., Schmidt, M. W. I., Smernik, R. J., Currie, L. A., Ball, W. P., Nguyen, T. H., et al. (2007). Comparison of quantification methods to measure fire-derived (black/elemental) carbon in soils and sediments using reference materials from soil, water, sediment and the atmosphere. *Global Biogeochemical Cycles*, 21, GB3016. <https://doi.org/10.1029/2006GB002914>
- Han, Y. M., Cao, J. J., An, Z. S., Chow, J. C., Watson, J. G., Jin, Z. D., et al. (2007). Evaluation of the thermal/optical reflectance method for quantification of elemental carbon in sediments. *Chemosphere*, 69(4), 526–533. <https://doi.org/10.1016/j.chemosphere.2007.03.035>
- Han, Y. M., Cao, J. J., Yan, B. Z., Kenna, T. C., Jin, Z. D., Cheng, Y., et al. (2011). Comparison of elemental carbon in lake sediments measured by three different methods and 150-year pollution history in eastern China. *Environmental Science & Technology*, 45(12), 5287–5293. <https://doi.org/10.1021/es103518c>
- Hu, L., Lin, T., Shi, X., Yang, Z., Wang, H., Zhang, G., & Guo, Z. (2011). The role of shelf mud depositional process and large river inputs on the fate of organochlorine pesticides in sediments of the yellow and East China seas. *Geophysical Research Letters*, 38, L03602. <https://doi.org/10.1029/2010GL045723>
- Hu, L., Shi, X., Bai, Y., Qiao, S., Li, L., Yu, Y., et al. (2016). Recent organic carbon sequestration in the shelf sediments of the Bohai Sea and Yellow Sea, China. *Journal of Marine Systems*, 155, 50–58. <https://doi.org/10.1016/j.jmarsys.2015.10.018>
- Huang, G., Chen, Y., Tian, C., Tang, J., Zhang, H., Luo, Y., et al. (2016). Spatial distributions and seasonal variations of dissolved black carbon in the Bohai Sea, China. *Journal of Coastal Research*, 74(sp1), 214–227. <https://doi.org/10.2112/si74-019.1>
- Huang, L., Zhang, J., Wu, Y., & Wang, J. (2016). Distribution and preservation of black carbon in the East China Sea sediments: Perspectives on carbon cycling at continental margins. *Deep Sea Research Part II: Topical Studies in Oceanography*, 124, 43–52. <https://doi.org/10.1016/j.dsr2.2015.04.029>
- Jaffé, R., Ding, Y., Niggemann, J., Vähätalo, A. V., Stubbins, A., Spencer, R. G. M., et al. (2013). Global charcoal mobilization from soils via dissolution and riverine transport to the oceans. *Science*, 340(6130), 345–347. <https://doi.org/10.1126/science.1231476>
- Jiang, X., Chen, Y., Tang, J., Huang, G., Liu, D., Li, J., & Zhang, G. (2010). The distribution of black carbon in the surface sediments of coastal zone, Bohai Bay (in Chinese). *Ecology and Environmental Sciences*, 19(7), 1617–1621.
- Kang, Y., Wang, X., Dai, M., Feng, H., Li, A., & Song, Q. (2009). Black carbon and polycyclic aromatic hydrocarbons (PAHs) in surface sediments of China's marginal seas. *Chinese Journal of Oceanology and Limnology*, 27(2), 297–308. <https://doi.org/10.1007/s00343-009-9151-x>
- Li, Y., Zhang, H., Tu, C., Fu, C., Xue, Y., & Luo, Y. (2016). Sources and fate of organic carbon and nitrogen from land to ocean: Identified by coupling stable isotopes with C/N ratio. *Estuarine, Coastal and Shelf Science*, 181, 114–122. <https://doi.org/10.1016/j.ecss.2016.08.024>
- Liu, K. K., Atkinson, L., Quinones, R., & TalaueMcManus, L. (2010). *Carbon and nutrient fluxes in continental margins: A global synthesis*. Berlin: Springer. <https://doi.org/10.1007/978-3-540-92735-8>
- Masiello, C., & Louchouart, P. (2013). Fire in the ocean. *Science*, 340(6130), 287–288. <https://doi.org/10.1126/science.1237688>
- Menon, S., Hansen, J., Nazarenko, L., & Luo, Y. (2002). Climate effects of black carbon aerosols in China and India. *Science*, 297(5590), 2250–2253. <https://doi.org/10.1126/science.1075159>
- Peng, J., Hu, M., Guo, S., Du, Z., Zheng, J., Shang, D., et al. (2016). Markedly enhanced absorption and direct radiative forcing of black carbon under polluted urban environments. *Proceedings of the National Academy of Sciences of the United States of America*, 113(16), 4266–4271. <https://doi.org/10.1073/pnas.1602310113>
- Qin, Y., Zheng, B., Lei, K., Lin, T., Hu, L., & Guo, Z. (2011). Distribution and mass inventory of polycyclic aromatic hydrocarbons in the sediments of the south Bohai Sea, China. *Marine Pollution Bulletin*, 62(2), 371–376. <https://doi.org/10.1016/j.marpolbul.2010.09.028>
- Ramanathan, V., & Carmichael, G. (2008). Global and regional climate changes due to black carbon. *Nature Geoscience*, 1(4), 221–227. <https://doi.org/10.1038/ngeo156>
- Sánchez-García, L., Cato, I., & Gustafsson, Ö. (2012). The sequestration sink of soot black carbon in the Northern European Shelf sediments. *Global Biogeochemical Cycles*, 26, GB1001. <https://doi.org/10.1029/2010GB003956>
- Santin, C., Doerr, S. H., Preston, C. M., & Gonzalez-Rodriguez, G. (2015). Pyrogenic organic matter production from wildfires: A missing sink in the global carbon cycle. *Global Change Biology*, 21(4), 1621–1633. <https://doi.org/10.1111/gcb.12800>
- Stubbins, A., Niggemann, J., & Dittmar, T. (2012). Photo-lability of deep ocean dissolved black carbon. *Biogeosciences*, 9(5), 1661–1670. <https://doi.org/10.5194/bg-9-1661-2012>
- Tan, S. C., Shi, G.-Y., & Wang, H. (2012). Long-range transport of spring dust storms in Inner Mongolia and impact on the China seas. *Atmospheric Environment*, 46(Supplement C), 299–308. <https://doi.org/10.1016/j.atmosenv.2011.09.058>

- Wang, R., Tao, S., Wang, W., Liu, J., Shen, H., Shen, G., et al. (2012). Black carbon emissions in China from 1949 to 2050. *Environmental Science & Technology*, *46*(14), 7595–7603. <https://doi.org/10.1021/es3003684>
- Wang, X., Ma, H., Li, R., Song, Z., & Wu, J. (2012). Seasonal fluxes and source variation of organic carbon transported by two major Chinese rivers: The Yellow River and Changjiang (Yangtze) River. *Global Biogeochemical Cycles*, *26*, GB2025. <https://doi.org/10.1029/2011GB004130>
- Wang, X., Xu, C., Druffel, E. R. M., Xue, Y., & Qi, Y. (2016). Two black carbon pools transported by the Changjiang and Huanghe Rivers in China. *Global Biogeochemical Cycles*, *30*, 1778–1790. <https://doi.org/10.1002/2016GB005509>
- Wang, Z., Pan, X., Uno, I., Li, J., Wang, Z., Chen, X., et al. (2017). Significant impacts of heterogeneous reactions on the chemical composition and mixing state of dust particles: A case study during dust events over northern China. *Atmospheric Environment*, *159*, 83–91. <https://doi.org/10.1016/j.atmosenv.2017.03.044>
- Wiedemeier, D. B., Hilf, M. D., Smittenberg, R. H., Haberer, S. G., & Schmidt, M. W. I. (2013). Improved assessment of pyrogenic carbon quantity and quality in environmental samples by high-performance liquid chromatography. *Journal of Chromatography A*, *1304*, 246–250. <https://doi.org/10.1016/j.chroma.2013.06.012>
- Xu, C., Xue, Y., Qi, Y., & Wang, X. (2016). Quantities and fluxes of dissolved and particulate black carbon in the Changjiang and Huanghe rivers, China. *Estuaries and Coasts*, *39*(6), 1617–1625. <https://doi.org/10.1007/s12237-016-0122-0>
- Yang, Y., Fang, J., Ma, W., Smith, P., Mohammad, A., Wang, S., & Wang, W. E. I. (2010). Soil carbon stock and its changes in northern China's grasslands from 1980s to 2000s. *Global Change Biology*, *16*(11), 3036–3047. <https://doi.org/10.1111/j.1365-2486.2009.02123.x>
- Yang, Z., Ji, Y., Bi, N., Lei, K., & Wang, H. (2011). Sediment transport off the Huanghe (Yellow River) delta and in the adjacent Bohai Sea in winter and seasonal comparison. *Estuarine, Coastal and Shelf Science*, *93*(3), 173–181. <https://doi.org/10.1016/j.ecss.2010.06.005>
- Zhang, L. J., Wang, L., Cai, W. J., Liu, D. M., & Yu, Z. G. (2013). Impact of human activities on organic carbon transport in the Yellow River. *Biogeosciences*, *10*(4), 2513–2524. <https://doi.org/10.5194/bg-10-2513-2013>
- Zhang, P., Song, J., & Yuan, H. (2009). Persistent organic pollutant residues in the sediments and mollusks from the Bohai Sea coastal areas, North China: An overview. *Environment International*, *35*(3), 632–646. <https://doi.org/10.1016/j.envint.2008.09.014>
- Zhang, S., Gan, W.-B., & Ittekkot, V. (1992). Organic matter in large turbid rivers: The Huanghe and its estuary. *Marine Chemistry*, *38*(1-2), 53–68. [https://doi.org/10.1016/0304-4203\(92\)90067-K](https://doi.org/10.1016/0304-4203(92)90067-K)
- Zhang, X. Y., Gong, S. L., Zhao, T. L., Arimoto, R., Wang, Y. Q., & Zhou, Z. J. (2003). Sources of Asian dust and role of climate change versus desertification in Asian dust emission. *Geophysical Research Letters*, *30*(24), 2272. <https://doi.org/10.1029/2003gl018206>
- Ziolkowski, L. A., Chamberlin, A. R., Greaves, J., & Druffel, E. R. M. (2011). Quantification of black carbon in marine systems using the benzene polycarboxylic acid method: A mechanistic and yield study. *Limnology and Oceanography: Methods*, *9*(4), 140–140. <https://doi.org/10.4319/lom.2011.9.140>